A Molecular Dynamics Simulation of a Bubble Nucleation on Solid Surface

Shigeo Maruyama and Tatsuto Kimura

Department of Mechanical Engineering, The University of Tokyo
7-3-1 Hongo, Bunkyo-ku, Tokyo 113-8656, Japan
E-mail: maruyama@photon.t.u-tokyo.ac.jp

ABSTRACT

A heterogeneous nucleation of a vapor bubble on a solid surface was simulated by the molecular dynamics method. Liquid argon between parallel solid surfaces was gradually expanded, until a vapor bubble was nucleated. Argon liquid was represented by 5488 Lennard-Jones molecules and each surface was represented by three layers of harmonic molecules with the constant temperature heat bath model. With a visualization of void patterns, the density fluctuations leading to the nucleation were compared for different wettability of the surface. The wettability was varied by changing the potential between argon and solid molecule. The over-all shape of the vapor bubble or the "contact angle" was measured at the equilibrium condition achieved after the expansion.

NOMENCLEATURE

H_c: Center of fitting circle, Å
h: Height, Å
k: Spring constant, N/m
k_B: Boltzmann constant, J/K
m: Mass, kg
N: Number of molecules
p: Pressure, MPa
$R_{1/2}$: Radius of fitting circle, Å
r: Radius, Å
or distance of two molecules, Å
T: Temperature, K
V: Volume, m^3

Greek Symbols

α: Damping factor, kg/s
Δt: Time Step, s
ε: Energy parameter of Lennard-Jones potential, J
ϕ: Potential function
θ: Contact angle, rad
σ: Length parameter of Lennard-Jones potential, Å
σ_F: Standard deviation of exciting force

Subscripts

AR: Argon
BOT: Bottom surface
DNS: Density profile
INT: Interaction between argon and solid molecules
i, j: Index of molecule
POT: Potential profile
S: Solid molecule
SURF: Integrated for surface
TOP: Top surface

1. INTRODUCTION

Microscopic understandings of phase interfaces have been badly anticipated in theories of traditional macroscopic heat transfer such as condensation coefficient in dropwise condensation, maximum heat transfer in boiling heat transfer, surface tension of a cluster in nucleation theory, and contact angle for the heat transfer of three-phase interface. Furthermore, recent advanced technologies introduced new microscopic problems in heat transfer such as droplet formation in the chemical vapor deposition process and a vapor bubble formation due to the intense laser heating. In order to understand the molecular level phenomena related to the phase-change heat transfer, we have been performing molecular dynamics simulations of liquid-vapor interface of a liquid droplet [1], contact of liquid droplet on a surface [2], and evaporation and condensation of liquid droplets on solid surface [3]. In this paper, a vapor bubble nucleation on a solid surface closely related to the cavitation and boiling phenomena was considered by the molecular dynamics method.

We used simple Lennard-Jones molecules for liquid and vapor molecules and further employed the Lennard-Jones function for the interaction potential between fluid and solid molecules. The solid molecules were represented by harmonic molecules with a temperature control using the phantom molecules. By gradually expanding the solid walls to the negative pressure, we could observe the formation of vapor bubble on the surface. The dynamic behavior of liquid density fluctuations leading to the bubble formation was studied by visualizing the low density patches of liquid. Then, the equilibrium shape of the vapor bubble attached to the surface was considered. The measured contact angle was in good agreement with the case of liquid droplet in contact with the surface [2,3].

2. MOLECULAR DYNAMICS SIMULATION

A heterogeneous nucleation of a vapor bubble on a solid surface was simulated by the molecular dynamics method. As shown in Figure 1, liquid argon consisted of 5488 molecules between parallel solid surfaces was prepared. The potential between argon molecules was represented by the well-known Lennard-Jones (12-6) function as

$$\phi(r) = 4\varepsilon \left[\left(\frac{\sigma}{r} \right)^{12} - \left(\frac{\sigma}{r} \right)^{6} \right] \tag{1}$$

where the length scale σ_{AR} = 3.40 Å, energy scale ε_{AR} = 1.67×10^{-21} J, and mass m_{AR} = 6.63×10^{-26} kg. We used the potential cut-off at $3.5\sigma_{AR}$ with the shift of the function for the continuous decay. Even though we could regard the system as Lennard-Jones fluid by the non-dimensional form, here we pretended that it was argon for the sake of physical understanding. The liquid argon was sandwiched by top and bottom

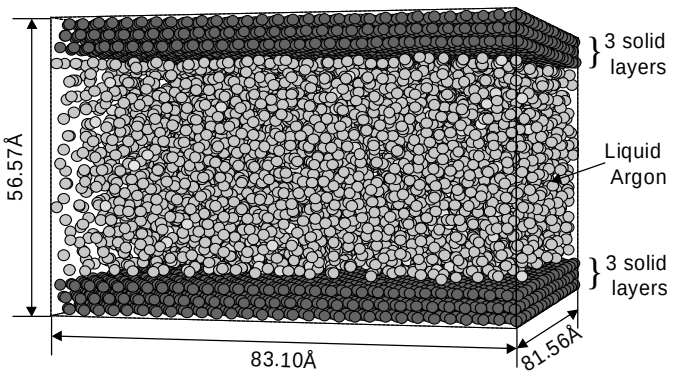

Figure 1. A snapshot of liquid argon between parallel solid surfaces.

solid surfaces, with periodic boundary conditions in four side surfaces.

The solid surface was represented by 3 layers of harmonic molecules (1020 molecules in each layer) in fcc (111) surface. Here, we set as: mass m_S = 3.24×10^{-25} kg, distance of nearest neighbor molecules σ_S = 2.77 Å, the spring constant k = 46.8 N/m, from the physical properties of solid platinum crystal. However, we regarded the solid as a simple insulating material because the effect of free electron and the accurate interaction potential between the metal atom and fluid atom were not explored yet. We have controlled the temperature of the solid surface by arranging a layer of phantom molecules outside of 3 layers. The phantom molecules modeled the infinitely wide bulk solid kept at a constant temperature T with proper heat conduction characteristics [4,5]. In practice, a solid molecule in the 3rd layer was connected with a phantom molecule with a spring of 2k and a damper of α = 5.184x10^{-12} kg/s in vertical direction and springs of 3.5k and dampers of α in two horizontal directions. A phantom molecule was further excited by the random force of gaussian distribution with the standard deviation

$$\sigma_F = \sqrt{\frac{2\alpha k_B T}{\Delta t}} \tag{2}$$

where k_B is Boltzmann constant. This technique mimicked the constant temperature heat bath which conducted heat from and to the 3rd layer as if a bulk solid was connected.

The potential between argon and solid molecule was also represented by the Lennard-Jones potential function with various energy scale parameter ε_{INT}. The length scale of the interaction potential σ_{INT} was kept constant as (σ_S+σ_{AR})/2 = 3.085 Å. In our previous study on the liquid droplet on the surface [2, 3], we have found that the depth of the integrated effective surface potential ε_{SURF} was directly related to the wettability of the surface. Hence, we used a quite wettable potential parameter (ε_{INT} = 1.009×10^{-21} J for 100 K and ε_{INT} = 1.009×10^{-21} J for 110 K) on the top surface to prevent from bubble nucleation and changed the wettability on the bottom surface as in Table 1. The solid surface became more wettable from E2 to E5 for 100 K and E2H to E5H for 110 K.

The classical momentum equation was integrated by the Verlet's leap-frog method with the time step of 5 fs. As an initial condition, an argon fcc crystal was placed at the center of the calculation domain of 83.10×81.56×56.57 Å^3 as in Figure 1 (the domain size was 83.10×81.56×58.57 Å^3 for 110 K). We used the velocity-scaling temperature-control directly to argon molecules for initial 100 ps. Then, switching off the direct temperature control, the system was run for 500 ps with the temperature control from the phantom molecules until the equilibrium argon liquid was achieved. Then, we gradually expanded the system volume by moving the top surface at a constant speed of 5 Å/ns (0.5 m/s). We could observe the bubble formation and growth. When we measured the equilibrium

Table 1. Calculation Conditions

Label	T_C (K)	ε_{INT}^{TOP} (×10^{-21}J)	ε_{INT}^{BOT} (×10^{-21}J)	$\varepsilon^*_{SURF}{}^{BOT}$	θ_{DNS} (deg)	θ_{POT} (deg)
E2	100	1.009	0.527	1.86	100.7	100.7
E3	100	1.009	0.688	2.42	68.8	66.7
E4	100	1.009	0.848	2.99	23.3	19.7
E5	100	1.009	1.009	3.56	-	-
E2H	110	0.894	0.467	1.65	118.7	117.1
E3H	110	0.894	0.610	2.15	82.7	78.1
E4H	110	0.894	0.752	2.65	60.2	53.4
E5H	110	0.894	0.894	3.15	-	-

shape of the vapor bubble, we picked up the time where the vapor bubble was well established as the initial condition and repeated the calculation for 500 ps without the expansion of the volume.

3. FORMATION OF VAPOR BUBBLE

After the equilibrium of liquid between two solid surfaces at desired temperature was obtained, we slowly expanded the surfaces in the constant temperature condition imposed by the phantom molecules. According to the increase in volume, the decrease of pressure was observed as in Figure 2. Here, we defined two different schemes for the evaluation of pressure. One is the direct measurement of force acting on solid surface molecules, denoted as "Wall Pressure" in Figure 2. Another is the extension of the virial representation. The virial pressure for two-body potential system is expressed as

$$p = \frac{Nk_BT}{V} - \frac{1}{6V}\left\langle \sum_{i,j} \overline{\mathbf{r}_{ij} grad_i \phi(r_{ij})} \right\rangle \quad (3)$$

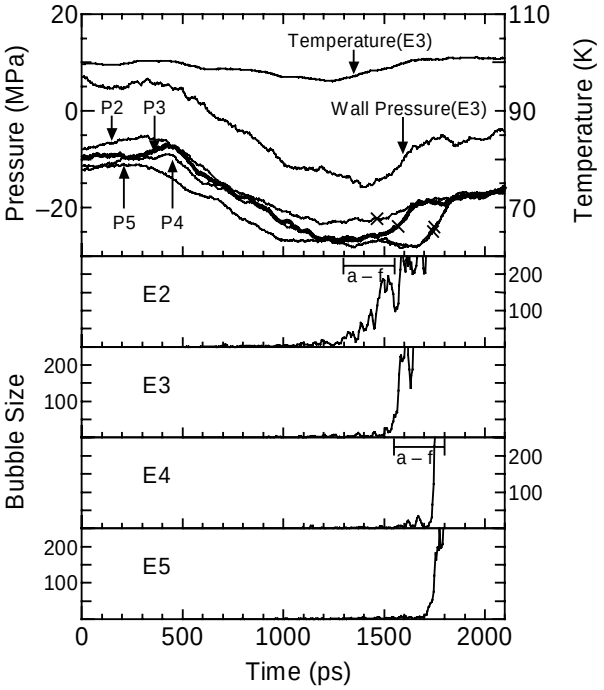

Figure 2. Pressure, temperature and bubble size variations for T = 100 K.

where the virial internal term should be summed for all molecule pairs inside the control volume. This summation is often extended to the outside of the periodic boundary conditions to evaluate the pressure value from a small calculation volume [6]. Even though this extension to the infinite system is physically questionable [7], we applied this scheme to compare with the well defined phase diagram of Lennard-Jones system [8].

The pressure variation showed a broad minimum after the expansion and we could observe the formation of vapor bubble in this time range. It seemed that the pressure recovery was related to the bubble growth. In order to visualize the density variations leading to the vapor bubble nucleation, we have applied three-dimensional grids of 2Å intervals and visualized the grid as a 'void' when there were no molecules within $1.2\sigma_{AR}$. An example of such a void view representation is shown in Figure 3(b) in comparison with the instantaneous sliced view (Figure 3(a)), which is the well established vapor bubble. Obviously, the assemble of such voids

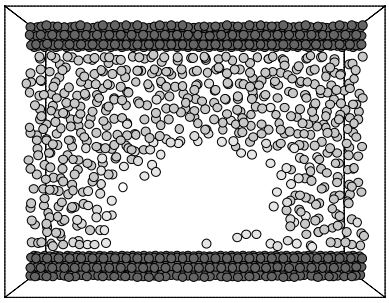

(a) Sliced View

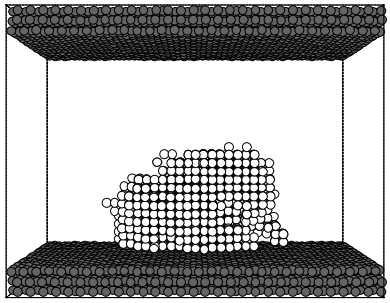

(b) Void View

Figure 3. A snapshot of a vapor bubble at 2100 ps for E3.

effectively represents the real void in the liquid. We have traced fluctuations of local density with this instantaneous void view.

Figure 4 shows an example of snapshots for the least wettable condition (E2; see our web site for the motion picture [9]). There appeared patches of liquid where the local density

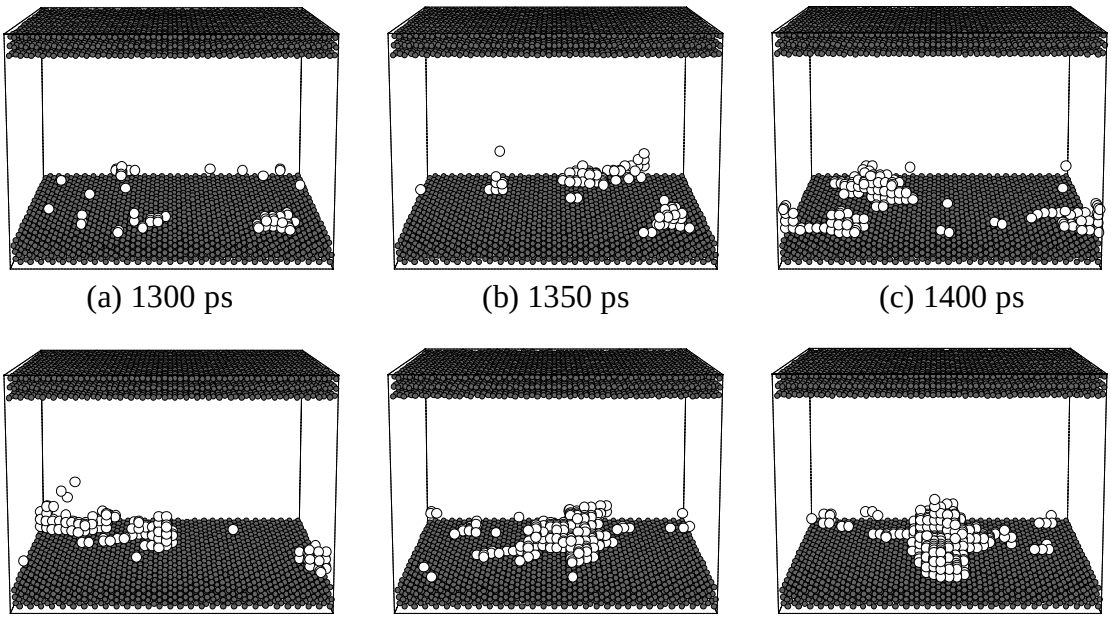

(a) 1300 ps (b) 1350 ps (c) 1400 ps

(d) 1450 ps (e) 1500 ps (f) 1550 ps

Figure 4. Snapshots of void patterns for E2.

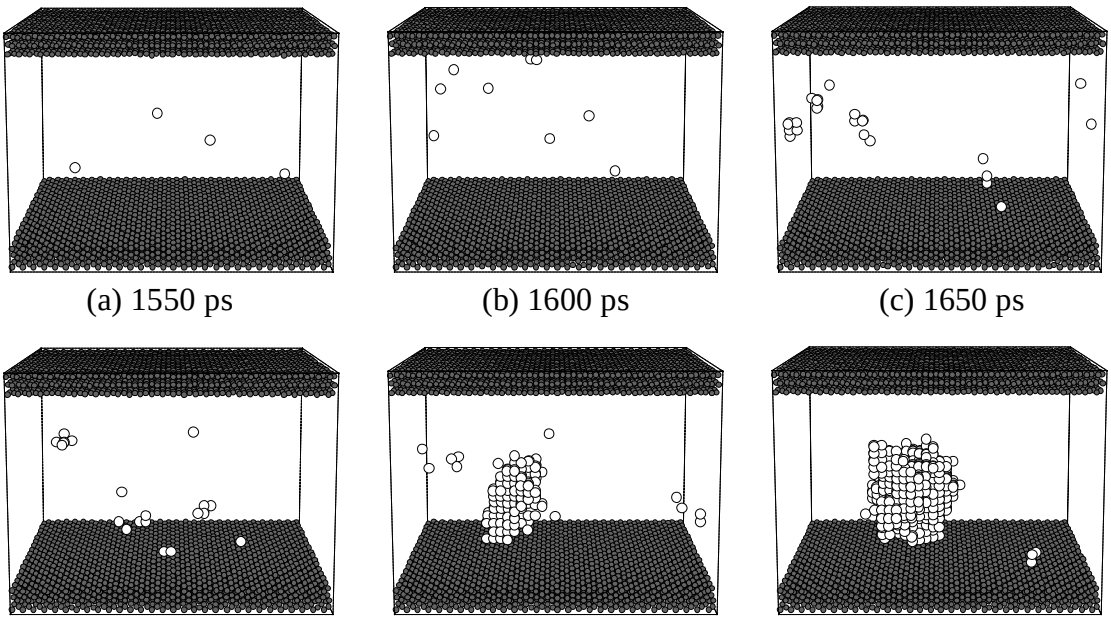

(a) 1550 ps (b) 1600 ps (c) 1650 ps

(d) 1700 ps (e) 1750 ps (f) 1800 ps

Figure 5. Snapshots of void patterns for E4 (Wettable surface).

was considerably low. These patches appeared and disappeared randomly in space and time but preferentially near the bottom surface. Finally, one of the patches successfully grew to a stable vapor bubble on the bottom solid surface where the lower wettability helped to sustain the nucleated bubble. It seems that when the void size is as large as 100 voids (related to about the radius of 10 Å), a single stable vapor bubble stayed on the surface. Another example of the density fluctuations for more wettable surface is shown in Figure 5. Here, no stable large void appeared until the sudden formation of the bubble in Figure 5(e) (see also Figure 2). It can be regarded that the bottom surface was not helpful enough to maintain the intermediate voids.

The size of the largest void in each snapshot is drawn in Figure 2 as "Bubble Size" in comparison with the pressure variations. When the bottom surface is less wettable, the size of void seems to increase monotonically, however, each void appeared and disappeared randomly in space. On the other hand, when the bottom surface is more wettable, no large void appeared until the sudden appearance of the void of about more that 100. We defined the nucleation point when the size of void exceeds 100.

We compared the nucleation pressure for various surface potential conditions (wettability) in temperature-pressure diagram in Figure 6. With the increase in the surface wettability, the nucleation pressure approached to the spinodal line (the thermodynamic limit of the existence of superheated liquid, calculated by the molecular dynamics method [8]). The result of the homogeneous nucleation simulation [10] is also plotted in the figure. When a very high wettability of the surface was employed, the situation was closer to the homogeneous nucleation as for E4 and E5. With the decrease in the wettability, the nucleation point moved farther from the spinodal line. These trends are very much in good agreement with the macroscopic concept that the less wettable surface helps the nucleation on the surface.

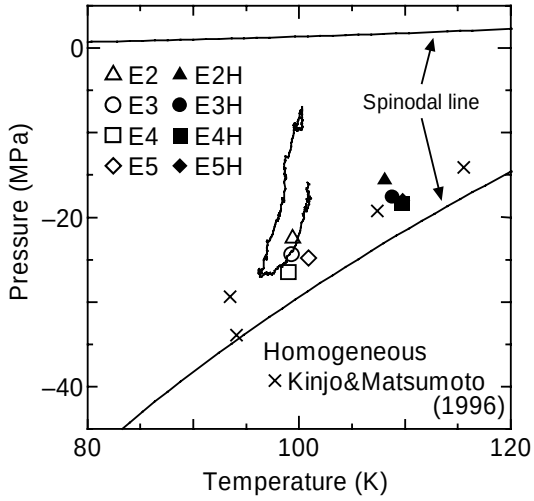

Figure 6. Pressure and temperature variations.

4. EQUILIBRIUM SHAPE OF VAPOR BUBBLE (CONTACT ANGLE)

After detecting the stable vapor bubble formed on the surface, we repeated the simulation for 500 ps without the volume expansion in order to observe the equilibrium structure of the vapor bubble. The two-dimensional density distributions shown in Figure 7 are obtained by cylindrical averaging through the center of the bubble. The layered structure of liquid near the surface is clearly observed. On the other hand, except for about two layers near the surface the shape of bubble can be considered to be a part of a sphere. It is observed that the less wettable surface leads to more flattered shape. Compared with the density profile, the potential profile in Figure 8 had no layered structure near the liquid-solid interface. These features of the vapor bubble are just the reversed image of our previous

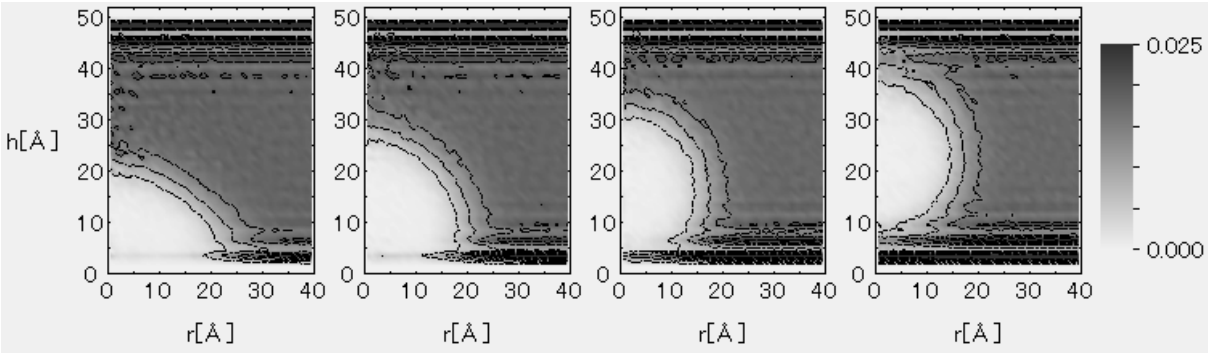

(a) E2 (b) E3 (c) E4 (d) E5

Figure 7. Two-dimensional density distributions.

MD simulation of a liquid droplet near the solid surface. We have measured the apparent contact angle by the least square fit of a circle to the density contour line of half of liquid density. Since we have discovered that the $\cos\theta$ was a linear function of the depth of integrated effective surface potential $\varepsilon^*_{SURF} = \varepsilon_{SURF} / \varepsilon_{AR}$ for the liquid droplet on the surface [3], we have compared the present result with the same fashion in Figure 9. It is obvious that the contact angle was in good agreement with the case of liquid droplet marked as cross symbols [2,3]. The effect of temperature was small that we could not determine from Figure 9. The slight deviation of the bubble system from the droplet system for larger ε^*_{SURF} is probably due to the employment of Lennard-Jones cut-off for the bubble system.

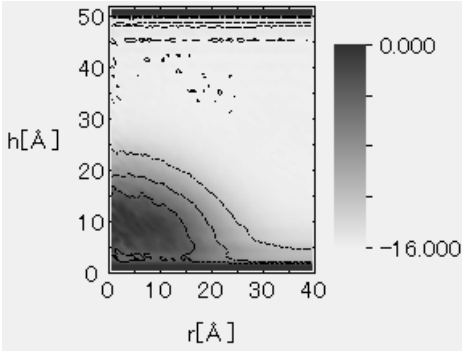

Figure 8. Two-dimensional potential distribution for E3.

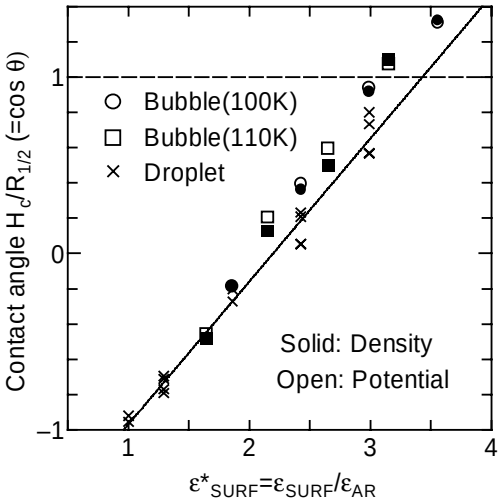

Figure 9. Contact angle correlated with ε^*_{SURF}.

It is interesting to consider the most wettable surface in Figure 7(d) (E5), in which it is clearly observed that the layered liquid structure completely covered the surface. In Figure 7 it seems that the bubble was just in the middle of two surfaces. However, a slightly smaller bubble in Figure 10 clearly shows that the bubble is still trapped on one of the surfaces. As we monitored the position of the center of bubble, it stayed at almost the same height from the bottom surface, though the ε_{INT} parameter on both surfaces were the same for this condition E5H. Even though the effect of the top surface might be concerned because the vertical calculation domain is limited, it is confirmed that the bubble was trapped by the bottom surface. Furthermore, if we extend the definition of the contact angle $\cos\theta$ to $H_c / R_{1/2}$, the measured point is almost on the line in Figure 9. Here, $R_{1/2}$ is

the radius of the fitting circle to the half-density contour, and H_c is the center of the fitting circle. This suggests the possibility of characterizing the liquid-solid contact beyond the apparent contact angle.

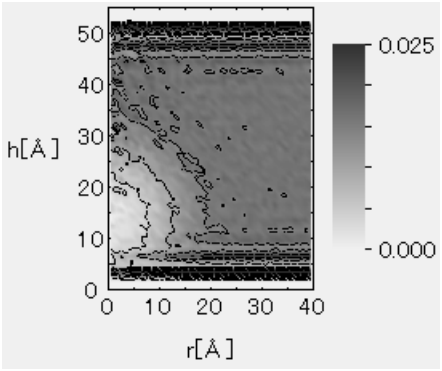

Figure 10. Equilibrium vapor bubble shape for E5H.

5. CONCLUSION

We have successfully demonstrated the nucleation of a 3-dimensional vapor bubble on the solid surface using the molecular dynamics method. The equilibrium shape of the vapor bubble was characterized by the potential parameter just in the same fashion as in the liquid droplet on the solid surface. Furthermore, dynamic behaviors of the low-density patches leading to the bubble nucleation were visualized for several wettability conditions.

REFERENCES

[1] Maruyama, S.. Matsumoto, S.. Ogita, A., Surface Phenomena of Molecular Clusters by Molecular Dynamics Method, Thermal Science Engineering, vol.2-1, pp.77-88 (1994).
[2] Matsumoto, S.. Maruyama, S.. Saruwatari, H., A Molecular Dynamics Simulation of a Liquid Droplet on a Solid Surface, Proc. ASME/JSME Thermal Engineering Joint Conf., Maui, vol.2, pp.557-562 (1995).
[3] Maruyama, S. et al., Liquid Droplet in Contact with a Solid Surface, Microscale Thermophysical Engineering, vol.2-1, pp.49-62 (1998).
[4] Tully, J.C., Dynamics of Gas-Surface Interactions: 3D Generalized Langevin Model Applied to fcc and bcc Surfaces, J. Chem. Phys., vol.73-4, pp.1975-1985 (1980).
[5] Blömer, J.. Beylich, A.E., MD-Simulation of Inelastic Molecular Collisions with Condensed Matter Surfaces, Proc. 20th Int. Symp. on Rarefied Gas Dynamics, Beijing, pp.392-397 (1997).
[6] Allen, M.P.. Tildesley, D.J., Computer Simulation of Liquids, Oxford University Press, Oxford, (1987).
[7] Iwaki, T., Molecular Dynamics Simulation of Thermal Stress during Rapid Solidification, Trans. JSME, Ser.A, vol.62-593 (1996).
[8] Nicolas, J.J. et al., Equation of State for the Lennard-Jones Fluid, Molecular Physics, vol.37-5, pp.1429-1454 (1979).
[9] http://www.photon.t.u-tokyo.ac.jp/~maruyama/bubble/index.html
[10] Kinjo, T.. Matsumoto, M., MD Simulation of the Inception of Vapor Phase in Lennard-Jones Luquids, Proc. ICHMT Symp., vol.1, pp.215-221 (1996).